Available online at www.sciencedirect.com
SCIENCE DIRECT®
PERGAMON
International Journal of Heat and Mass Transfer 46 (2003) 2005–2014
International Journal of HEAT and MASS TRANSFER
www.elsevier.com/locate/ijhmt

Solution of radiative heat transfer in a semitransparent slab with an arbitrary refractive index distribution and diffuse gray boundaries

He-Ping Tan *, Yong Huang *, Xin-Lin Xia

School of Energy Science and Engineering, Harbin Institute of Technology, 92 West Dazhi Str., Harbin, Heilongjiang 150001, China

Received 18 October 2002

Abstract

On the basis of medium discretization and local linear approximation of refractive index distribution, the curved ray tracing technique is used in combination with the pseudo source adding method to numerically solve the radiative heat transfer in a semitransparent slab with an arbitrary refractive index distribution and two diffuse gray walls. The radiative equilibrium temperature field of a linear refractive index distribution is evaluated by this method and the results show excellent agreement with that of the previous research. For two types of sinusoidal refractive index distributions, the radiative equilibrium temperature field as well as the temperature and heat flux fields of coupled radiation–conduction are investigated in detail. The results show considerable significance of the gradient refractive index effect, and some important conclusions are to be obtained.

Keywords: Radiation transfer; Gradient refractive index; Semitransparent medium; Curved ray tracing technique; Pseudo source adding method

1. Introduction

The radiative heat transfer in a gradient refractive index medium can be found in many technology processes, such as the heating of glass and thermal protecting coatings, the manufacturing of waveguide materials, the ray transporting through atmosphere, as well as the optical measurement of flame and other semitransparent medium. But the investigation on such heat transfer in a gradient refractive index medium has not been found until recent years. In 2000, Ben Abdallah and Le Dez put forward a curved ray tracing technique to solve the radiation transfer in a gradient refractive index medium, and first analyzed the thermal emission of a semitransparent slab with variable spatial refractive index [1]. By this method, they also investigated the radiation transfer and coupled radiation–conduction inside a semitransparent slab with variable spatial refractive index [2,3], as well as the thermal emission of a two-dimensional rectangular cavity [4]. In 2002, Xia and Huang et al. analyzed the thermal emission and volumetric absorption of a graded index semitransparent medium layer by a ray splitting and tracing technique [5], and resorting to a pseudo source adding method to deal with the radiative intensity on boundary surfaces, the curved ray tracing technique is used to solve the radiation transfer and the couple radiation–conduction in a gradient refractive index slab with gray boundaries [6,7]. Also in 2002, Lemonnier and Le Dez presented a discrete ordinate solution of radiative transfer across a slab with variable refractive index [8]. All these researches have show the considerable effect of gradient refractive index on radiation transfer in medium.

In this paper, the radiative heat transfer in an absorbing-emitting semitransparent slab with an arbitrary

* Corresponding authors. Tel.: +86-451-641-2148.
E-mail address: huangy_zl@263.net (Y. Huang).

0017-9310/03/$ - see front matter
doi:10.1016/S0017-9310(02)00502-1

Nomenclature

a_k	coefficient denoting the influence of temperature of sublayer k on $I^-(0,\xi)$
A_k	coefficient denoting the influence of temperature of sublayer k on I_{01}
b, b'	coefficients denoting the influence of sublayer temperature on $I(z_j,\xi)$and $I(z_j,-\xi)$, respectively
B_{kj}, B'_{kj}	coefficients defined in Eqs. (27) and (28), respectively
c_k	coefficient denoting the influence of temperature of sublayer k on $I^+(d,\xi)$
C_k	coefficient denoting the influence of temperature of sublayer k on I_{d1}
D_{kj}	coefficients defined in Eq. (36)
d	slab thickness, m
I	radiative intensity, W/m^2 sr
$I^*(j)$	reduced radiative intensities ($n=1$) at the jth splitting point, W/m^2 sr
K_{ij}	influencing factor denote the coupling influence of the two boundaries
L	number of discrete angles of the hemispherical space
$n(z)$	refractive index distribution
$\tilde{n}(z)$	linear approximation of refractive index distribution in a sublayer
M	number of sublayers
N	radiative–conductive parameter, $N=\lambda\kappa/(4\sigma n_R^2 T_R^3)$, $n_R=(n_{max}+n_{min})/2$
q	heat flux density, W/m^2
q^*	dimensionless heat flux, $q^*=q/q_R$, $q_R=\sigma T_R^4$
$s(j)$	curve length of the propagating route between two tracing points
T	temperature, K
T_R	reference temperature, $T_R=(T_0+T_d)/2$, K
z	space coordinate, m
Δz	sublayer thickness, m

Greek symbols

ε	emissivity of boundary wall
ζ	angle between the ray propagating direction and the interface normal
κ	absorption coefficient, m^{-1}
λ	thermal conductivity, W/m K
ξ	polar angle of propagating direction
σ	Stefan–Boltzmann constant, 5.729×10^{-8} W/m^2 K^4
τ	optical thickness, $\tau=\kappa d$
Ω	spatial direction

Superscripts and subscripts

$+,-$	direction from boundary 2 to boundary 1 (−) or from boundary 1 to boundary 2 (+)
c	conduction
d	position of $z=d$
j, k	sublayer order
0	position of $z=0$
p	pseudo source
r	radiation
t	total radiation and conduction

refractive index distribution and diffuse gray boundaries is to be solved numerically. For two types of sinusoidal refractive index distributions, the radiation transfer and coupled radiation–conduction are analyzed in detail.

2. Geometrical and physical model

Consider an infinite parallel plane slab of absorbing–emitting but non-scattering gray medium of thickness d, as shown in Fig. 1. The emissivities of the two diffuse gray boundary walls are ε_0 and ε_d , and the temperatures are T_0 and T_d, respectively. The medium is characterized by a constant absorption coefficient κ, a constant thermal conductivity λ and a refractive index distribution $n(z)$. A steady state temperature field $T(z)$ will be caused by the coupled radiation–conduction in medium. Radiation will dominate the heat transfer process if the thermal conductivity λ is small enough, and the temperature field would be a radiative equilibrium one thereby.

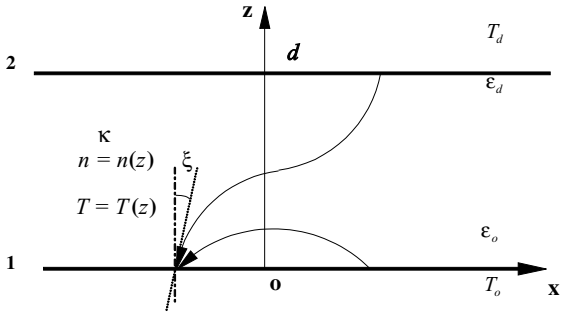

Fig. 1. Schematic diagram of geometrical and physical model.

3. Discretization and solution

3.1. Discretization

As shown in Fig. 2, the medium is divided into $M-2$ isothermal sublayers of equal thickness Δz. The two

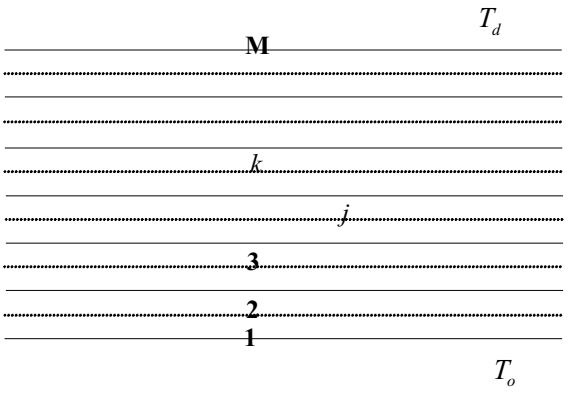

Fig. 2. Discretization of the slab.

boundary walls are regarded as the sublayers of zero thickness, and named as the first sublayer and the Mth one, respectively. The temperature of a sublayer k in medium, with center z_k, is denoted by T_k. The refractive index distribution $n(z)$ within a sublayer is substituted by a linear approximation $\tilde{n}(z)$, as

$$\tilde{n}(z) = n(z_k - \Delta z/2) + \frac{z - z_k + \Delta z/2}{\Delta z}[n(z_k + \Delta z/2) - n(z_k - \Delta z/2)], \quad (1)$$

where, $2 \leqslant k \leqslant M-1$, and $(k-2)\Delta z \leqslant z \leqslant (k-1)\Delta z$.

3.2. Solution of radiative intensities leaving gray boundaries

The radiative intensity leaving a gray boundary is the combination of boundary emission and reflection. It can be solved by employing the pseudo source adding method in combination with the curved ray tracing technique. The solution can be divided into the following steps.

(i) Deduce the radiative intensity reaching a boundary without considering the boundary emission and reflection.

Take the solution of radiative intensity reaching the boundary 1 as an example, which is denoted by $I^-(0,\xi)$. By tracing the trajectory of a curved ray propagating in the reverse direction of ξ , a series of recursion relations can be deduced [1–3,6,7], which are

$$\frac{I^-(0,\xi)}{n^2(0)} = \frac{\sigma T_2^4}{\pi}\left[1 - e^{-\kappa s(1)}\right] + I^*(1)e^{-\kappa s(1)}, \quad (2)$$

$$I^*(j) = \frac{\sigma T_l^4}{\pi}\left[1 - e^{-\kappa s(j+1)}\right] + I^*(j+1)e^{-\kappa s(j+1)} \quad (j = 1, 2, 3, \ldots), \quad (3)$$

where T_2 is the temperature of the second sublayer, T_l is that of the lth sublayer located from jth to $(j+1)$th tracing point, and $s(j+1)$ is the curve length of the propagating route accordingly.

Two typical propagating trajectories for the curved ray tracing have been shown in Fig. 3. The ray tracing process is ended when a boundary surface is reached or the influence of radiative intensity $I^*(j+1)$ on $I^-(0,\xi)$ can be neglectable, and the value of $I^*(j+1)$ is set to be zero. Resorting to the previous analysis on the propagating route of a ray in a linear refractive index medium [6,7], the following equations can be gained to evaluate the curve length between two adjacent tracing points, i.e. for $n' \sin\zeta_{\text{out}} < n''$,

$$s(j+1) = \frac{\Delta z}{n'' - n'}\left(\sqrt{n''^2 - n'^2 \sin^2\zeta_{\text{out}}} - n'\cos\zeta_{\text{out}}\right),$$

$$\zeta_{\text{in}} = \arcsin(n'\zeta_{\text{out}}/n'') \quad (4)$$

and for $n' \sin\zeta_{\text{out}} \geqslant n''$,

$$s(j+1) = \frac{2\Delta z n' \cos\zeta_{\text{out}}}{n' - n''},$$

$$\zeta_{\text{in}} = \zeta_{\text{out}}, \quad (5)$$

where n' is the refractive index value at the boundary 1 or the jth tracing point, n'' is that at the other interface of the sublayer which the ray is propagating through, and ζ is the angle between the propagating direction of the ray and the interface normal at a tracing point. The subscript 'out' denotes the current tracing point, and 'in' denotes the next one.

It can be seen from the above equations, that $I^-(0,\xi)$ is a function of the sublayer temperatures, which can be written as

$$\frac{I^-(0,\xi)}{n^2(0)} = \frac{\sigma}{\pi}\sum_{k=2}^{M-1} a_k T_k^4, \quad (6)$$

where a_k is a coefficient denoting the influence of the temperature of sublayer k on $I^-(0,\xi)$, and it is evaluated by the numerical summing in the curved ray tracing process.

Similarly, without considering the boundary emission and reflection, the expression for calculating the radiative intensity reaching the boundary 2 can be deduced, which is

$$\frac{I^+(d,\xi)}{n^2(d)} = \frac{\sigma}{\pi}\sum_{k=2}^{M-1} c_k T_k^4, \quad (7)$$

where c_k is a coefficient denoting the influence of the temperature of sublayer k on $I^+(d,\xi)$, and it is also evaluated by the numerical summing in the curved ray tracing process.

(ii) Take account of the boundary reflection and emission

The reflected energy by a diffuse gray wall will mix together with the radiative energy emitted by it.

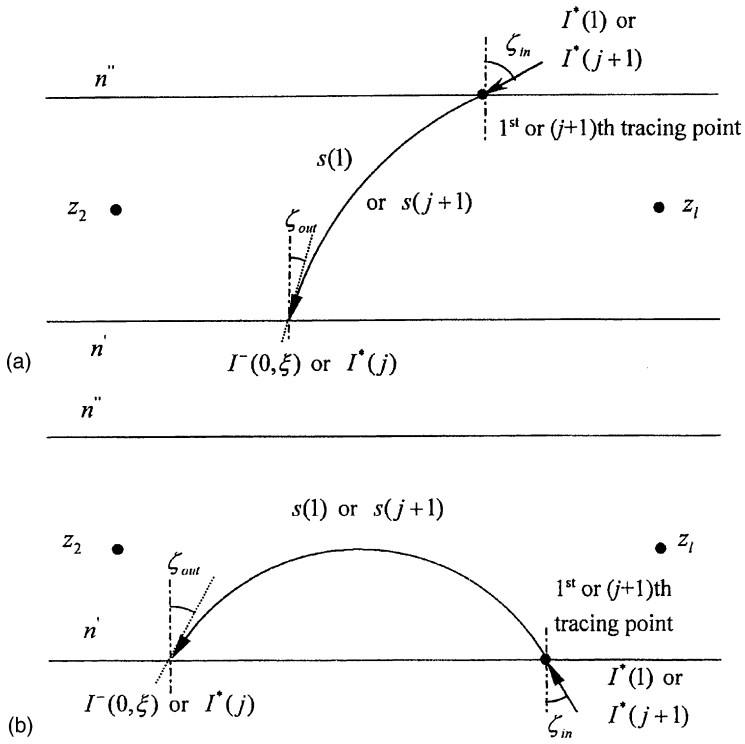

Fig. 3. Schematic diagram of the curved ray tracing process.

Introduce the mixed radiative intensities I_{01} and I_{d1} for the two boundaries respectively, which are defined by the following equations.

$$I_{01} = 2(1-\varepsilon_0)\int_0^{\pi/2} I^{-}(0,\xi)\sin\xi\cos\xi\,\mathrm{d}\xi + n^2(0)\varepsilon_0\sigma T_0^4/\pi, \tag{8}$$

$$I_{d1} = 2(1-\varepsilon_d)\int_0^{\pi/2} I^{+}(d,\xi)\sin\xi\cos\xi\,\mathrm{d}\xi + n^2(d)\varepsilon_d\sigma T_d^4/\pi. \tag{9}$$

Resorting to Eq. (6), the integral term in Eq. (8) can be solved and expressed as

$$\int_0^{\pi/2} I^{-}(0,\xi)\sin\xi\cos\xi\,\mathrm{d}\xi = \frac{\sigma n^2(0)}{\pi}\sum_{i=1}^{L}\sum_{k=2}^{M-1} a_k T_k^4 \sin\xi_i\cos\xi_i\frac{\pi}{2L}, \tag{10}$$

where L is the number of discrete angles of the hemispherical space, and ξ_i is the discrete direction, $\xi_i = (i-0.5)\pi/2L$. So, Eq. (8) can be reformed as

$$I_{01} = \frac{\sigma n^2(0)}{\pi}\sum_{k=1}^{M} A_k T_k^4, \tag{11}$$

where $T_1 = T_0$, $T_M = T_d$, $A_1 = \varepsilon_0$, $A_M = 0$.

Similarly, Eq. (9) can be reformed as

$$I_{d1} = \frac{\sigma n^2(d)}{\pi}\sum_{k=1}^{M} C_k T_k^4, \tag{12}$$

where $C_1 = 0$, $C_M = \varepsilon_d$.

Obviously, only the once reflection and the emission of the boundary surface is included in I_{01} or I_{d1}, and the influence of the other boundary is not considered. So, I_{01} and I_{d1} are not the real radiative intensities leaving the boundaries. They are named as the radiative intensities of the first pseudo sources.

(iii) Take account of the coupling influence of the two boundaries.

If the medium refractive index is constant, the radiative energy from a boundary cannot propagate back to it before being reflected by the other boundary. In a gradient refractive index medium, however, the inner total refraction will lead to this phenomenon. So, the radiative energy leaving a boundary can partly reach the other boundary and partly return back after propagating in the gradient refractive index medium. An influencing factor K_{ij} is introduced to denote the coupling influence of the two boundaries. It refers to the percentage of radiative energy arriving at the boundary j in all of the radiative energy leaving the boundary i. By

tracing the propagating process of a curved ray leaving a boundary, the expressions for calculating K_{ij} can be deduced, such as

$$K_{12} = 2\sum_{i=1}^{m} \exp\left[-\kappa\sum_{j=1}^{N_i} s(j)\right] \sin\xi_i \cos\xi_i \frac{\pi}{2L}, \tag{13}$$

$$K_{11} = 2\sum_{i=m+1}^{L} \exp\left[-\kappa\sum_{j=1}^{N_i} s(j)\right] \sin\xi_i \cos\xi_i \frac{\pi}{2L}, \tag{14}$$

where m is the number of rays arriving at the boundary 2, $L-m$ is that returning to the boundary 1, and N_i is the number of sublayers which the curved ray i has propagated through. The similar equations can be obtained for K_{21} and K_{22}.

(iv) Deduce the radiative intensities leaving the two boundaries.

After propagating through the medium, the radiative energy of the first pseudo sources at the boundary 1 and that at the boundary 2 can partly reach the boundary 1 to be reflected diffusely. And the reflected energy is named as the second pseudo source emission of the boundary 1. Similarly, the second pseudo source emission of the boundary 2 is defined. Their radiative intensities are calculated by the following equations.

$$I_{02} = (1-\varepsilon_0)(K_{11}I_{01} + K_{21}I_{02}), \tag{15}$$

$$I_{d2} = (1-\varepsilon_d)(K_{12}I_{01} + K_{22}I_{02}). \tag{16}$$

By the same way, a series of pseudo source emission can be defined for a boundary, and the sum of the radiative intensities of a pseudo source series is just the real radiative intensity leaving the boundary. So, the radiative intensities leaving the two boundaries are

$$I_0 = I_{01} + I_{02} + I_{03} + \cdots, \tag{17}$$

$$I_d = I_{d1} + I_{d2} + I_{d3} + \cdots. \tag{18}$$

By considering Eqs. (11,12,15,16), the above two equations can be reformed as

$$I_0 = \frac{\sigma n^2(0)}{\pi}\sum_{k=1}^{M} \frac{A_k + \frac{C_k K_{21}(1-\varepsilon_0)n^2(d)}{[1-K_{22}(1-\varepsilon_d)]n^2(0)}}{1-(1-\varepsilon_0)\left[K_{11} + \frac{K_{12}K_{21}(1-\varepsilon_d)}{1-K_{22}(1-\varepsilon_d)}\right]} T_k^4 = \frac{\sigma n^2(0)}{\pi}\sum_{k=1}^{M} A'_k T_k^4, \tag{19}$$

$$I_d = \frac{\sigma n^2(d)}{\pi}\sum_{k=1}^{M} \frac{C_k + \frac{A_k K_{12}(1-\varepsilon_d)n^2(0)}{[1-K_{11}(1-\varepsilon_0)]n^2(d)}}{1-(1-\varepsilon_d)\left[K_{22} + \frac{K_{21}K_{12}(1-\varepsilon_0)}{1-K_{11}(1-\varepsilon_0)}\right]} T_k^4 = \frac{\sigma n^2(d)}{\pi}\sum_{k=1}^{M} C'_k T_k^4. \tag{20}$$

It can be seen that, I_0 and I_d equal to the radiative intensities emitted from two black walls with temperatures T_{p0} and T_{pd}, respectively, which are

$$T_{p0}^4 = \sum_{k=1}^{N} A'_k T_k^4, \quad T_{pd}^4 = \sum_{k=1}^{N} C'_k T_k^4. \tag{21}$$

By the deduction and analysis above, the solution of radiative transfer in a gradient refractive index medium with two diffuse gray boundaries is transformed into that with black boundaries, and the radiative intensities leaving boundaries are solved.

3.3. Solution of temperature field at radiative equilibrium

At radiative equilibrium, the heat transfer in medium is only by radiation, and under the steady state, the radiative energy isotropically emitted from any infinitesimal volume of the medium equals to that directionally absorbed over the whole space. Thus the energy balance equation is

$$4n^2(s)\sigma T^4(s) = \int_{\Omega=4\pi} I(s,\Omega)\,\mathrm{d}\Omega, \tag{22}$$

where $I(s,\Omega)$ is the radiative intensity of medium at position s and in direction Ω. For the slab, the azimuthal symmetry leads to

$$\int_{\Omega=4\pi} I(s,\Omega)\,\mathrm{d}\Omega = 2\pi\int_0^{\pi/2} [I(z,\xi) + I(z,-\xi)]\sin\xi\,\mathrm{d}\xi. \tag{23}$$

For any sublayer j with center z_j, similar to that in Section 3.2, we can deduce equations to calculate the radiative intensities $I(z_j,\xi)$ and $I(z_j,-\xi)$ as

$$\frac{I(z_j,\xi)}{n^2(z_j)} = \frac{\sigma}{\pi}\left(\sum_{k=2}^{M-1} b_k T_k^4 + b_1 T_{p0}^4 + b_M T_{pd}^4\right), \tag{24}$$

$$\frac{I(z_j,-\xi)}{n^2(z_j)} = \frac{\sigma}{\pi}\left(\sum_{k=2}^{M-1} b'_k T_k^4 + b'_1 T_{p0}^4 + b'_M T_{pd}^4\right), \tag{25}$$

where b_k and b'_k are coefficients denoting the influences of T_k.

The energy balance equation can thus be transformed into the following discrete form:

$$4n^2(z_j)\sigma T_j^4 = 2\sigma n^2(z_j)\sum_{i=1}^{L}\left[\sum_{k=2}^{M-1}(b_k + b'_k)T_k^4 + (b_1 + b'_1)T_{p0}^4 + (b_M + b'_M)T_{pd}^4\right]\sin\xi_i\frac{\pi}{2L}. \tag{26}$$

This can be reformed further as

$$T_k^4 = \sum_{j=2}^{M-1} B_{jk} T_j^4 + B_{1,k} T_{p0}^4 + B_{M,k} T_{pd}^4. \tag{27}$$

The discrete temperature field in medium can be finally given as

$$\begin{pmatrix} 1 & 0 & 0 & 0 & 0 \\ B'_{12} & 1+B'_{22}-\frac{B_{22}}{2} & B'_{32}-\frac{B_{32}}{2} & B'_{M-1,2}-\frac{B_{M-1,2}}{2} & B'_{M,2} \\ & & & & \\ B'_{1,M-1} & B'_{2,M-1}-\frac{B_{2,M-1}}{2} & & 1+B'_{M-1,M-1}-\frac{B_{M-1,M-1}}{2} & B'_{M,M-1} \\ 0 & 0 & & 0 & 1 \end{pmatrix} \begin{pmatrix} \Theta_1 \\ \Theta_2 \\ \\ \\ \Theta_{M-1} \\ \Theta_M \end{pmatrix} = \begin{pmatrix} T_0^4 \\ 0 \\ \\ \\ 0 \\ T_d^4 \end{pmatrix}, \tag{28}$$

where $\Theta = T^4$, $B'_{kj} = -\frac{1}{2}B_{1,j}C'_k - \frac{1}{2}B_{M,j}A'_k$.

The form of Eq. (28) is same as that in [6], but the solutions of coefficients B_{kj}, A'_k and C'_k are different. For a linear refractive index distribution considered in [6], they can be exactly solved, but for other refractive index distributions, they have to be solved numerically.

3.4. Solution of coupled radiation–conduction

For the coupled radiation–conduction in medium, the energy balance equation at a steady state is

$$\operatorname{div}(q_r + q_c) = 0, \tag{29}$$

where q_r and q_c are the heat fluxes transferred by radiation and conduction, respectively. For a one-dimensional problem, the divergences of them are

$$\operatorname{div} q_r = \kappa\left[4n^2(z)\sigma T^4(z) - 2\pi\int_0^{\pi/2}[I(z,\xi)+I(z,-\xi)]\sin\xi\,\mathrm{d}\xi\right], \tag{30}$$

$$\operatorname{div} q_c = -\lambda\frac{\mathrm{d}^2T}{\mathrm{d}z^2}. \tag{31}$$

For any sublayer j with center z_j, the discrete form of Eq. (30) can be deduced by the analysis similar to that of Eq. (24), which is

$$\begin{aligned}\operatorname{div} q_r = 4\kappa\sigma n_j^2\Bigg[&\left(1-\frac{B_{1j}C'_j}{2}-\frac{B_{Mj}A'_j}{2}-\frac{B_{jj}}{2}\right)T_j^4 \\ &-\frac{B_{1j}C'_1+B_{Mj}A'_1}{2}T_0^4-\frac{B_{1j}C'_M+B_{Mj}A'_M}{2}T_d^4 \\ &-\sum_{k=2}^{j-1}\frac{B_{1j}C'_k+B_{Mj}A'_k+B_{kj}}{2}T_k^4 \\ &-\sum_{k=j+1}^{M-1}\frac{B_{1j}C'_k+B_{Mj}A'_k+B_{kj}}{2}T_k^4\Bigg].\end{aligned} \tag{32}$$

By the finite difference method, Eq. (31) can be discretized as

$$\begin{aligned}&\operatorname{div} q_c = \lambda\frac{12T_2-8T_0-4T_3}{3\Delta z^2}, \quad \text{for } j=2 \\ &\operatorname{div} q_c = \lambda\frac{2T_j-T_{j-1}-T_{j+1}}{\Delta z^2}, \quad \text{for } 3\leqslant j\leqslant M-2 \\ &\operatorname{div} q_c = \lambda\frac{12T_{M-1}-4T_{M-2}-8T_d}{3\Delta z^2}, \quad \text{for } j=M-1.\end{aligned} \tag{33}$$

Substitute Eqs. (32) and (33) into Eq. (29) to get the discrete energy equation for sublayer j. By linearizing the T_j^4 term, it is transformed into an algebraic equation. And a set of algebraic equations can be obtained for all sublayers. By an iterative solution, the temperature field induced by coupled radiation–conduction in medium can be finally evaluated.

3.5. Radiative flux field of coupled radiation–conduction

The radiative flux field inside the slab can be expressed as

$$q_r(s) = \int_{\Omega=4\pi} I(s,\Omega)\Omega\,\mathrm{d}\Omega. \tag{34}$$

The azimuthal symmetry leads to

$$\int_{\Omega=4\pi} I(s,\Omega)\Omega\,\mathrm{d}\Omega = 2\pi\int_0^{\pi/2}[I(z,\xi)-I(z,-\xi)]\sin\xi\cos\xi\,\mathrm{d}\xi. \tag{35}$$

So for any sublayer j with center z_j, the following expression for evaluating the discrete radiative flux q_{rj} can be deduced.

$$\begin{aligned}q_{rj} &= 2\sigma n^2(z_j)\sum_{i=1}^{L}\left[\sum_{k=2}^{N-1}(b_k-b'_k)T_k^4+(b_1-b'_1)T_{p0}^4\right. \\ &\quad\left.+(b_N-b'_N)T_{pd}^4\right]\sin\xi_i\cos\xi_i\frac{\pi}{2L} \\ &= 2\sigma n^2(z_j)\left(\sum_{k=2}^{N-1}D_{kj}T_k^4+D_{1j}T_{p0}^4+D_{N,j}T_{pd}^4\right).\end{aligned} \tag{36}$$

4. Results and discussion

In the calculations below, the slab thickness and boundary temperatures keep constant, which are $d = 1.0$ cm, $T_0 = 1000$ K and $T_d = 1500$ K, respectively.

4.1. Temperature field at radiative equilibrium

The radiative equilibrium temperature field in a semitransparent slab with the linear refractive index distribution of $n(z) = 1.2 + 0.6z/d$ has been presented in [2,6]. It is also calculated by the numerical method in this paper, and the almost same results are obtained, as shown in Fig. 4.

In Fig. 5, the radiative equilibrium temperature fields under two kinds of sinusoidal refractive index distributions are shown, which are dashed lines for $n(z) = 1.2 + 0.6\sin(\pi z/d)$ and solid lines for $n(z) = 1.8 - 0.6\sin(\pi z/d)$. For a large range of optical thickness τ, a considerable difference can be found between the temperature fields of the two sinusoidal refractive index distributions, and it is significantly related to the emissivities of the two boundaries. For example, for a fixed optical thickness and a fixed couple of boundary emissivities, the maximum temperature difference in medium,

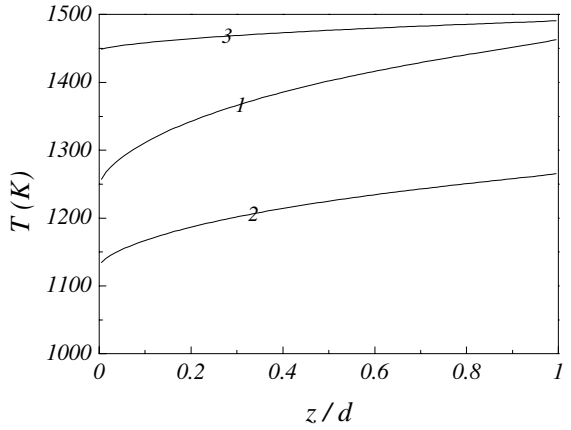

Fig. 4. Temperature field inside the slab at radiative equilibrium: $n(z) = 1.2 + 0.6z/d$. (1) $\varepsilon_1 = \varepsilon_2 = 1$; (2) $\varepsilon_1 = 1$, $\varepsilon_2 = 0.2$; (3) $\varepsilon_1 = 0.2$, $\varepsilon_2 = 1$.

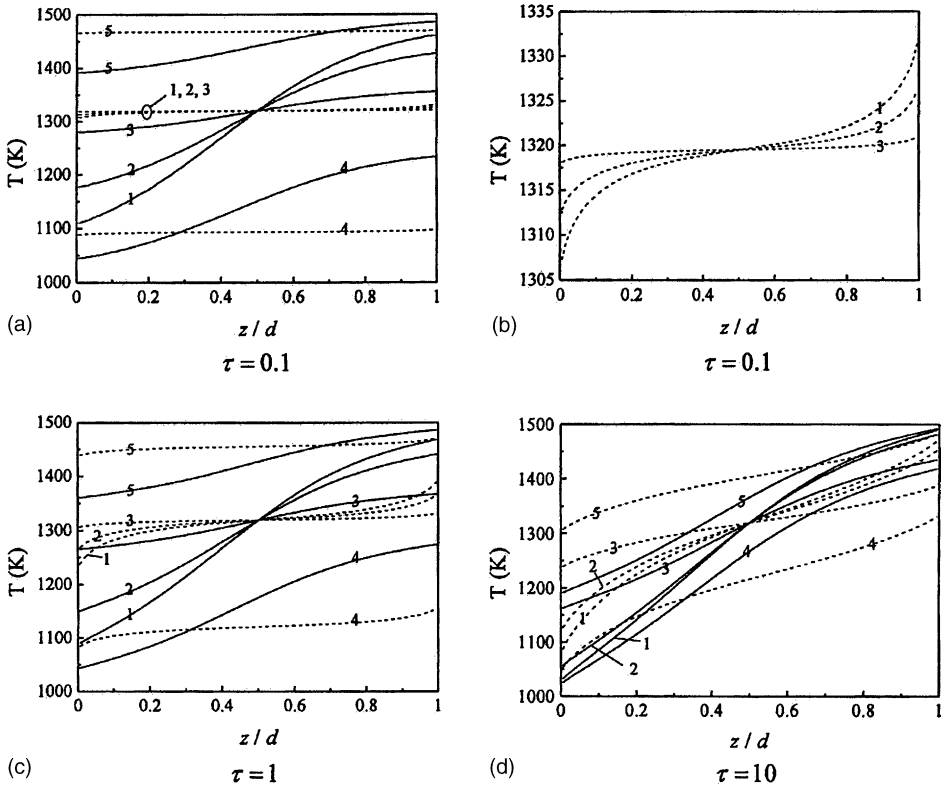

Fig. 5. Temperature field inside the slab at radiative equilibrium. (1) $\varepsilon_1 = \varepsilon_2 = 1$; (2) $\varepsilon_1 = \varepsilon_2 = 0.7$; (3) $\varepsilon_1 = \varepsilon_2 = 0.2$; (4) $\varepsilon_1 = 1$, $\varepsilon_2 = 0.2$; (5) $\varepsilon_1 = 0.2$, $\varepsilon_2 = 1$. Dashed lines: $n(z) = 1.2 + 0.6\sin(\pi z/d)$; solid lines: $n(z) = 1.8 - 0.6\sin(\pi z/d)$.

i.e. $T(d)-T(0)$, is much smaller for $n(z)=1.2+0.6\sin(\pi z/d)$ than for $n(z)=1.8-0.6\sin(\pi z/d)$. And for the refractive index distribution of $n(z)=1.2+0.6\sin(\pi z/d)$ and the optical thickness $\tau=0.1$, $T(d)-T(0)$ is about 25 K under two black boundaries, but only 5 K under two gray boundaries with emissivities of 0.2.

The influence of boundary emissivities is easy to understand. Because the two boundaries can be regarded as the black walls with temperature T_{p0} and T_{pd}, and $T(d)-T(0)$ is proportional to $(T_{pd}-T_{p0})$, which descends with the decrease of boundary emissivities.

The difference between the radiative equilibrium temperature fields of two kinds of sinusoidal refractive index distributions is mainly caused by the different characteristics of the radiation transfer. When the refractive index distribution is $n(z)=1.2+0.6\sin(\pi z/d)$, the rays leaving any boundary can reach the other one after being attenuated by medium, i.e. no total reflection occurs for these rays, and the influencing

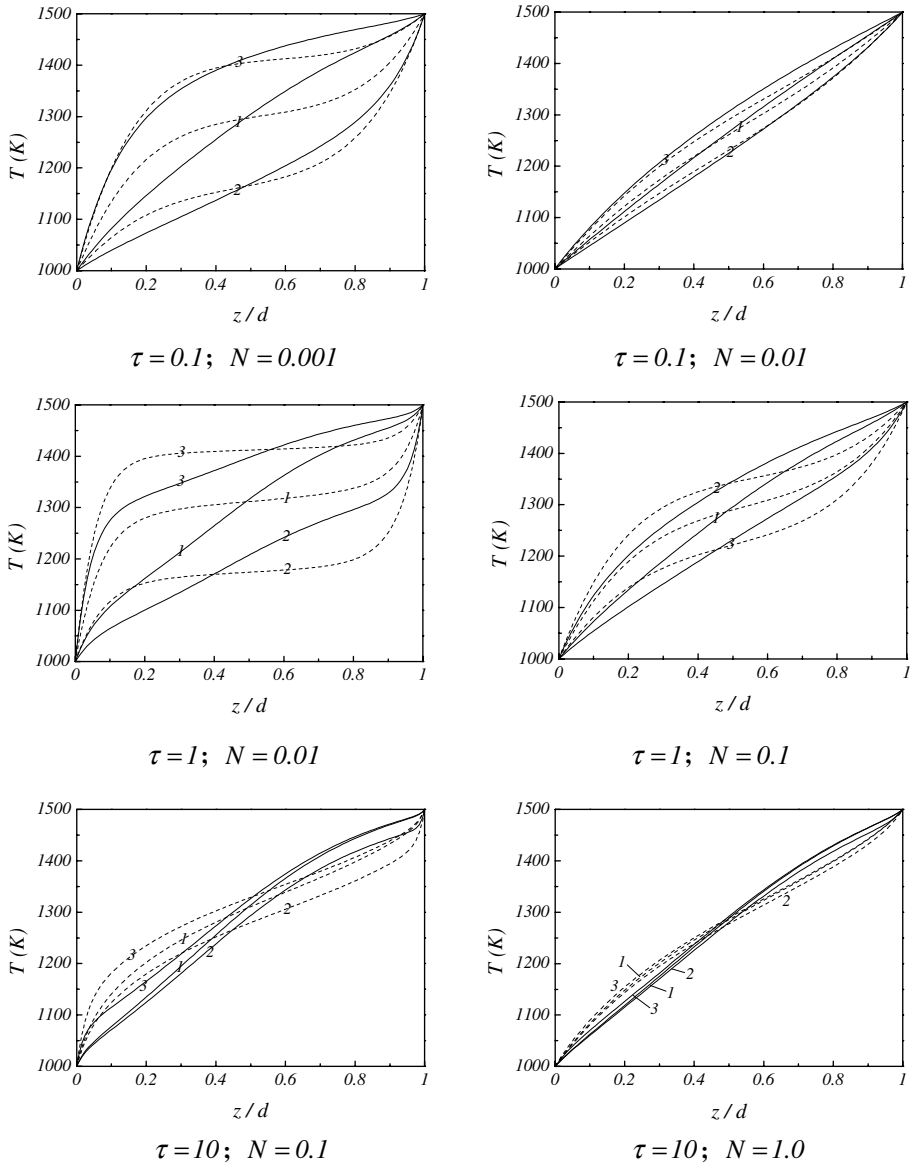

Fig. 6. Temperature field inside the slab at coupled radiation and conduction heat transfer. (1) $\varepsilon_1=\varepsilon_2=1$; (2) $\varepsilon_1=1$, $\varepsilon_2=0.2$; (3) $\varepsilon_1=0.2$, $\varepsilon_2=1$. Dashed lines: $n(z)=1.2+0.6\sin(\pi z/d)$; solid lines: $n(z)=1.8-0.6\sin(\pi z/d)$.

factors $K_{11} = 0$, $K_{22} = 0$. For the case of $n(z) = 1.8 - 0.6\sin(\pi z/d)$, however, the rays leaving a boundary will partly return back to it because of the total reflection, and $K_{11} \neq 0$, $K_{22} \neq 0$. So, in this case, compared with the former, the radiative energy is more difficult to be transferred from the high temperature boundary to the low temperature boundary, and this leads to a larger value of $T(d) - T(0)$. On the other hand, in the case of $n(z) = 1.2 + 0.6\sin(\pi z/d)$, the total reflection taking place near the middle of slab results in a more flat temperature distribution, as shown by the dashed lines in Fig. 5.

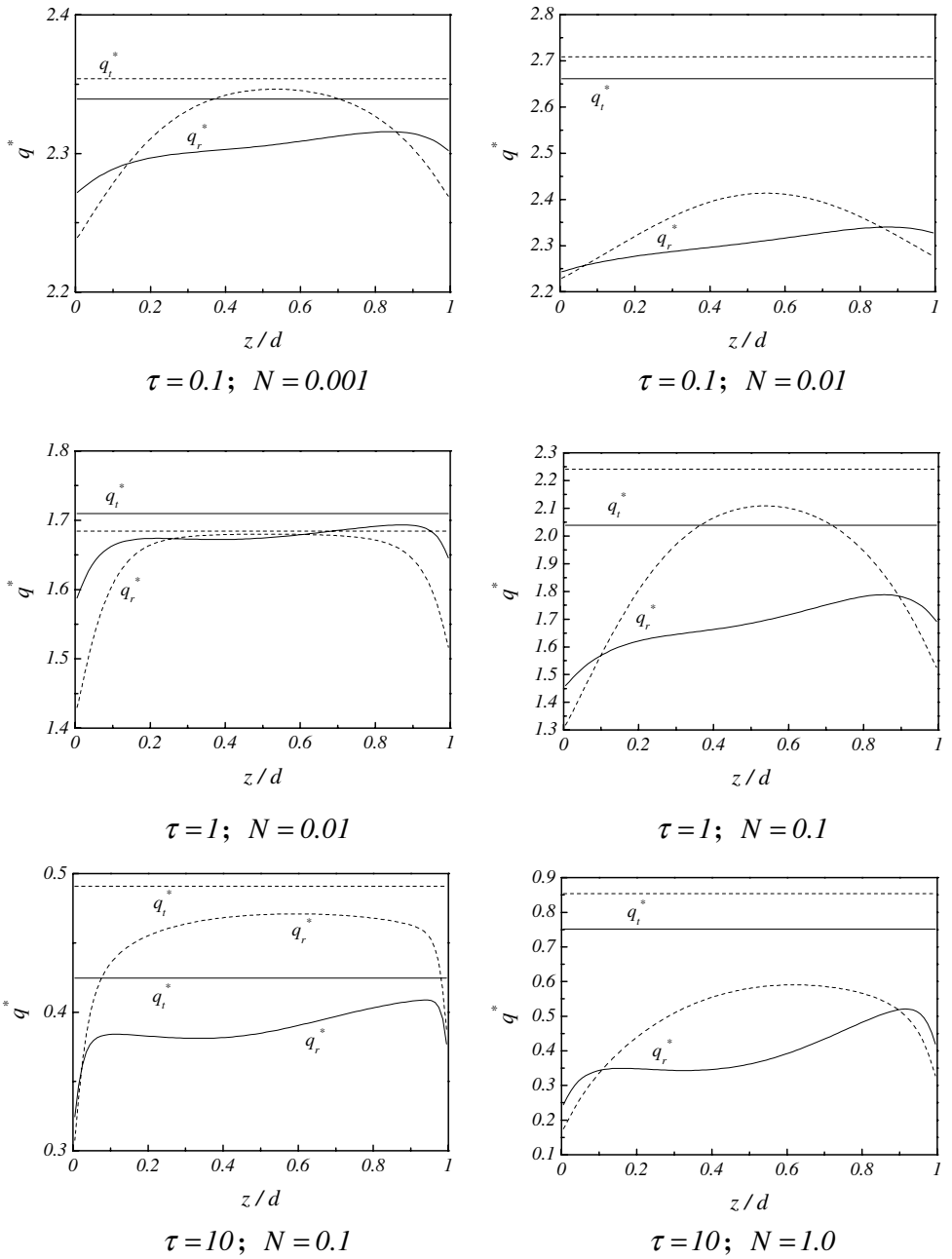

Fig. 7. Heat flux field inside the slab at coupled radiation–conduction ($\varepsilon_1 = \varepsilon_2 = 1$). Dashed lines: $n(z) = 1.2 + 0.6\sin(\pi z/d)$; solid lines: $n(z) = 1.8 - 0.6\sin(\pi z/d)$.

4.2. Temperature and heat flux of coupled radiation–conduction

The steady state coupled radiation–conduction heat transfer in a slab with the sinusoidal refractive index distribution is calculated, and the influences of optical thickness τ, radiative–conductive parameter N and the boundary emissivities are considered. The results of temperature field and heat flux are shown in Figs. 6 and 7, respectively.

For a moderate optical thickness and a small radiative–conductive parameter, such as $\tau = 1$ and $N = 0.01$, or $\tau = 0.1$ and $N = 0.001$, the radiation transfer plays the dominating role in the coupled heat transfer, accordingly, the temperature fields show great departure from the linear distribution, and the effect of refractive index distribution is significant (see Fig. 6). The temperature fields under the two sinusoidal refractive index distributions are quite different in these cases.

Because of the different characteristics of radiation transfer, the temperature of $n(z) = 1.2 + 0.6\sin(\pi z/d)$ (dashed lines), compared with that of $n(z) = 1.8 - 0.6\sin(\pi z/d)$ (solid lines), is lower in the adjacent region of high temperature boundary but higher in that of the other boundary, and becomes more flat in the main middle region. This is true whether the two boundaries are both black or one is black and the other gray.

When the high temperature boundary is gray, the temperature level in medium is lowered, and that will change contrarily if the low temperature boundary is gray. But the form of temperature curve does not change compared with that of two black boundaries (see Fig. 6).

Except for the case of $\tau = 1$ and $N = 0.01$ (see Fig. 7) for the most groups of optical thickness and radiative–conductive parameter, the total heat flux q_t of coupled heat transfer under $n(z) = 1.2 + 0.6\sin(\pi z/d)$ is larger than that under $n(z) = 1.8 - 0.6\sin(\pi z/d)$. The distributions of radiative heat flux q_r show great difference for the two sinusoidal refractive index distributions. For the case of $n(z) = 1.2 + 0.6\sin(\pi z/d)$, only one peak appears in a curve of q_r, but when the optical thickness is large enough, two peaks of q_r can be seen for the case of $n(z) = 1.8 - 0.6\sin(\pi z/d)$. It should be pointed out that, for a constant or linear refractive index distribution, the radiative heat flux of the coupled heat transfer shows only one peak [7].

5. Conclusion

The following conclusions can be drawn from this investigation.

1. The presented numerical method for solving the radiation transfer is flexible and reliable enough for an arbitrary refractive index distribution and diffuse gray boundaries.
2. The effect of gradient refractive index on radiation transfer is considerably significant within a large range of optical thickness, the temperature and heat flux fields can be quite different for two different refractive index distributions.
3. For the coupled radiation–conduction heat transfer in medium, a sinusoidal refractive index distribution can result in a complex radiative heat flux distribution with one or two peaks.
4. The boundary emissivities can greatly influence the temperature level in medium, but do not change the form of temperature curve.

Acknowledgements

The project is supported by the Fok Ying Tung Education Foundation (Grant No. 81050), and the National Natural Science Foundation of China (Grant No. 50076010). The authors are indebted to them for financial support.

References

[1] P. Ben Abdallah, V. Le Dez, Thermal emission of a semitransparent slab with variable spatial refractive index, J. Quant. Spectrosc. Radiat. Transfer 67 (3) (2000) 185–198.
[2] P. Ben Abdallah, V. Le Dez, Temperature field inside an absorbing-emitting semitransparent slab at radiative equilibrium with variable spatial refractive index, J. Quant. Spectrosc. Radiat. Transfer 65 (4) (2000) 595–608.
[3] P. Ben Abdallah, V. Le Dez, Radiative flux field inside an absorbing-emitting semitransparent slab with variable spatial refractive index at radiative conductive coupling, J. Quant. Spectrosc. Radiat. Transfer 67 (2) (2000) 125–137.
[4] P. Ben Abdallah, V. Le Dez, Thermal emission of a two-dimensional rectangular cavity with spatial affine refractive index, J. Quant. Spectrosc. Radiat. Transfer 66 (6) (2000) 555–569.
[5] X.L. Xia, Y. Huang, H.P. Tan, Thermal emission and volumetric absorption of a graded index semitransparent medium layer, J. Quant. Spectrosc. Radiat. Transfer 74 (2) (2002) 235–248.
[6] Y. Huang, X.L. Xia, H.P. Tan, Temperature fields inside an absorbing-emitting semi-transparent slab at radiative equilibrium with linear graded index and gray walls, J. Quant. Spectrosc. Radiat. Transfer 74 (2) (2002) 249–261.
[7] X.L. Xia, Y. Huang, H.P. Tan, Simultaneous radiation and conduction heat transfer in a graded index semitransparent slab with gray boundaries, Int. J. Heat Mass Transfer 45 (15) (2002) 2673–2688.
[8] D. Lemonnier, V. Le Dez, Discrete ordinates solution of radiative transfer across a slab with variable refractive index, J. Quant. Spectrosc. Radiat. Transfer 73 (2002) 195–204.